

Published in final edited form as:

Acta Biomater. 2012 October ; 8(10): 3695–3703. doi:10.1016/j.actbio.2012.06.030.

Injectable extracellular matrix derived hydrogel provides a platform for enhanced retention and delivery of a heparin-binding growth factor

Sonya B. Seif-Naraghi, Dinah Horn, Pam A. Schup-Magoffin, and Karen L. Christman*
University of California, San Diego, La Jolla, CA

Abstract

Injectable hydrogels derived from the extracellular matrix (ECM) of decellularized tissues have recently emerged as scaffolds for tissue engineering applications. Here, we introduce the potential for using a decellularized ECM-derived hydrogel for the improved delivery of heparin-binding growth factors. Immobilization of growth factors on a scaffold has been shown to increase their stability and activity. This can be done via chemical crosslinking, covalent bonding, or by incorporating natural or synthetic growth factor binding domains similar to those found *in vivo* in sulfated glycosaminoglycans (GAGs). Many decellularized ECM-derived hydrogels retain native sulfated GAGs and, therefore, these materials may provide an excellent delivery platform for heparin-binding growth factors. In this study, the sulfated GAG content of an ECM hydrogel derived from decellularized pericardial ECM was confirmed with FTIR and its ability to bind basic fibroblast growth factor (bFGF) was established. Delivery in the pericardial matrix hydrogel increased retention of bFGF both *in vitro* and *in vivo* in ischemic myocardium compared to delivery in collagen. In a rodent infarct model, intramyocardial injection of bFGF in pericardial matrix enhanced neovascularization by approximately 112% compared to delivery in collagen. Importantly, the newly formed vasculature was anastomosed with existing vasculature. Thus, the sulfated GAG content of the decellularized ECM hydrogel provides a platform for incorporation of heparin binding growth factors for prolonged retention and delivery.

1. Introduction

In many disease states – myocardial and peripheral ischemia, diabetic ulcers, retinal diseases, chronic wounds, etc. – the pathology is caused by a reduced blood supply [1]. This causes cell death in the downstream tissue, followed by degradation of the associated extracellular matrix. Tissue engineering approaches, designed to mitigate the damage and promote healing or regeneration, focus on eliciting angiogenesis and remodeling of the damaged region. This remodeling can be achieved by encouraging endogenous cell infiltration into an acellular biomaterial or by delivering exogenous cells; in both cases, the goal is to encourage repair and contribute to the function of the organ. In order to do this, many tissue engineering strategies have attempted to design materials to mimic the structure and composition of the native extracellular matrix (ECM) [2–5]. More recently, scaffolds

© 2012 Acta Materialia Inc. Published by Elsevier Ltd. All rights reserved.

*Corresponding Author: christman@eng.ucsd.edu, Tel: 858.534.9628, Fax: 858.534.2722.

Disclosure Statement

The authors have no competing financial interests to disclose.

Publisher's Disclaimer: This is a PDF file of an unedited manuscript that has been accepted for publication. As a service to our customers we are providing this early version of the manuscript. The manuscript will undergo copyediting, typesetting, and review of the resulting proof before it is published in its final citable form. Please note that during the production process errors may be discovered which could affect the content, and all legal disclaimers that apply to the journal pertain.

derived from the native ECM of decellularized tissues have been developed and used in tissue engineering applications [6–9]. These materials can be used intact as three-dimensional implantable scaffolds, as well as processed into injectable hydrogels that self-assemble *in situ*. When implanted or injected *in vivo*, previous work has demonstrated that these materials provide a template for cell infiltration and neovascularization [10–12]. In the case of cardiac repair, injectable ECM-derived hydrogels from decellularized small intestinal submucosa and the myocardium have been explored [7, 13, 14]. Injected alone into an infarct in small animals, these materials promote cell infiltration and have also been shown to preserve cardiac function post-myocardial infarction (MI) [13, 14]. While the mechanisms behind their effectiveness *in vivo* have yet to be fully elucidated, it is clear that ECM-derived hydrogels provide porous, fibrous scaffolds that allow for cellular infiltration and neovascularization in ischemic regions.

In addition to their use as biomaterial only therapies and cellular delivery platforms, tissue engineered scaffolds can also be used to deliver bioactive moieties such as growth factors. Therapeutic angiogenesis via administration of angiogenic factors, such as vascular endothelial growth factor (VEGF) and basic fibroblast growth factor (bFGF), has specifically been investigated in a variety of disease models including myocardial and peripheral ischemia [15–20], and wound repair [21–26]; a number of good reviews have been written on the topic [1, 27–29]. Restoring blood supply has been demonstrated to have positive effects; for example, using growth factors for cardiac repair has demonstrated that inducing angiogenesis may preserve endogenous cardiomyocytes and functionally contractile myocardium post-MI [30–32]. To harness this potential, growth factor delivery systems have been designed to deliver these proteins to infarcted tissue. Growth factors, such as VEGF and bFGF have been immobilized within delivery systems based on synthetic polymers such as poly(ethylene glycol) (PEG) [29, 33] and poly-NiPAam [34–36], as well as naturally derived polymers such as collagen [37, 38] and hyaluronic acid [27–29]. Other delivery systems involve self-assembling peptides [39] or hybrid materials. Most systems either incorporate biomolecules that associate with growth factors natively, such as heparin or heparan sulfate [40, 41] or use derivatives that include highly sulfated sugars [42] or heparin-like growth factor binding domains [43, 44]. Previous work has demonstrated the advantage of immobilization over physical entrapment or bolus injection, as it increases growth factor stability and localizes the effects to the site of treatment [45]. Unfortunately, the modifications used to increase growth factor activity or stability may change the chemistry of many natural biopolymers and therefore change their activity *in vivo* [46]. Natively, immobilization is achieved by the interaction between growth factors and sulfated glycosaminoglycans (sGAGs) that are bound to ECM proteins [47]. In this way, the ECM sequesters and presents growth factors within the tissue microenvironment.

Processed from native extracellular matrix, a variety of ECM-derived hydrogels have been shown to retain sGAG content [6–9]. As discussed, *in vivo*, the ECM sequesters growth factors; we therefore hypothesized that the sGAG content of decellularized ECM-derived hydrogels could provide a platform for enhanced retention and delivery of growth factors without additional material manipulation. While a variety of hybrid materials have been developed as growth factor delivery systems, the potential for using exogenous angiogenic factors incorporated in a decellularized ECM-derived hydrogel has yet to be investigated. To this end, we examined the delivery of a heparin-binding growth factor in a pericardial matrix hydrogel, which was recently developed as a potentially autologous scaffold for cardiac repair [8]. As a model system, we explored the delivery of bFGF in the ECM hydrogel in a rat myocardial infarction model. We demonstrate that the sGAG-containing ECM-derived hydrogel enhances retention and delivery of bFGF in ischemic myocardium via ionic association with the extant sugar content, resulting in increased retention and acute neovascularization when compared to delivery of the growth factor in collagen or saline.

2. Materials and Methods

All experiments in this study were performed in accordance with the guidelines published by the Institutional Animal Care and Use Committee at the University of California, San Diego, and the American Association for Accreditation of Laboratory Animal Care.

2.1 Tissue collection and decellularization

Porcine pericardia were collected from juvenile Yorkshire pigs and decellularized with sodium dodecyl sulfate (SDS), an ionic detergent previously shown to decellularize pericardium [8, 48]. After dissecting away any adherent adipose tissue, the samples were first washed in DI water for 30 min, and then stirred continuously in 1% SDS in PBS for 24 h, followed by an overnight DI rinse. Specimens were then removed from solution and agitated rinses under running DI water were performed to remove residual SDS. This protocol has previously demonstrated consistent decellularization of both human and porcine pericardial tissue samples [8, 49].

2.2 Preparation of injectable ECM and collagen hydrogels

Injectable ECM was prepared via methods modified from previously published protocols for bladder [9] and myocardial matrix [7]. Decellularized porcine pericardia were lyophilized and ground into a coarse powder with a Wiley mini mill (Thomas Scientific, Swedesboro, NJ). Milled samples were frozen and stored at -80°C until further use. When used, aliquots were pepsin-digested in 0.1 M HCl at a concentration of 10 mg ECM per 1 mL HCl. Pepsin (Sigma, St. Louis, MO) was used at a concentration of 1 mg/mL. The ECM powder was digested for 60–65 h and then brought to physiologic pH (7.4) and osmolarity (1x PBS) by adding 1 M NaOH (1/10 of original digest volume) and 10x PBS (1/10 of final neutralized volume). Raising the pH stops pepsin activity; the enzyme is deactivated above pH 6 [50]. All processing steps, including the pepsin digestion, were performed at room temperature. The resulting liquid was diluted with 1x PBS to the 6 mg/mL before use. For gels including growth factor, bFGF (GlobalStem, Rockville, MD) was added prior to dilution to the matrix such that the final 75 μL volume contained 10 μg of growth factor. Collagen gels were prepared from rat tail collagen type 1 (BD Biosciences). Collagen was used at a pH of 7.4 and a concentration of 2.5 mg/mL. All solutions were sterile-filtered before use and all manipulation was performed in a biosafety cabinet.

2.3 Comparison of mechanical and structural properties

Rheometry was used to verify that the PPM and collagen gels had similar mechanical properties at these concentrations. To do so, 350 μL gels were made from each material and tested on a parallel plate rheometer with a gap height of 0.8 mm. A frequency sweep was performed at 2.5% strain, a value previously determined to be within the linear region for these materials. The storage modulus was determined and compared; both are reported at 1 rad/s. Each gel was run in duplicate and three gels from each material were tested. Scanning electron microscopy was used to verify that the fiber density was similar. Gels were fixed in 2.5% glutaraldehyde (SigmaAldrich, Grade II, 25%, St Louis, MO) for 2 hours, dehydrated with a serial dilution of ethanol (30 – 100%), before being critical point dried in CO_2 using a Tousimis AutoSamdri 815A and sputter-coated with iridium using an Emitech K575X Sputter Coater. Samples were imaged with an FEI XL30 Ultra High Resolution Scanning Electron Microscope (UHR SEM) and images were taken at 2000x magnification. To compare fiber density, images were taken at 2,000x and the number of fibers that intersected two diagonal lines drawn across the image was quantified. This provided a method of comparing the two materials to each other and allowed us to determine if the fiber density was similar.

2.4 Confirmation and quantification of sulfated GAG content

Fourier transform infrared (FTIR) spectroscopy was performed to confirm the presence of carbohydrates in the material. Porcine pericardial matrix (PPM) and collagen samples were prepared as though for *in vivo* injections and then frozen and lyophilized. Transmission FTIR spectra were measured on a Nicolet Magna 550 spectrometer. An average of 64 scans were acquired, at a spectral resolution of 4 cm^{-1} . A background scan was obtained in the absence of material and the baseline was normalized for each sample after acquisition. Sulfated glycosaminoglycan (sGAG) content of the injectable ECM was quantified using a colorimetric Blyscan GAG assay (Biocolor, Carrickfergus, United Kingdom). Samples were run in triplicate.

2.5 *In vitro* retention and release

In order to evaluate if the ECM-derived hydrogel could sequester bFGF for prolonged release as compared to encapsulation in collagen, retention was first evaluated *in vitro*. Sets ($n = 6$) of $100\ \mu\text{L}$ PPM or collagen gels were formed overnight in microcentrifuge tubes. $10\ \mu\text{g}$ of bFGF was added to both materials before gelation. After gelation, the gels were rinsed to remove any bFGF not incorporated in the gels. After rinsing, $150\ \mu\text{L}$ of PBS was added to each sample. The supernatant was collected and exchanged every 24 hours for 5 days, at which point bacterial collagenase (Worthington Biomedical Corporation, Lakewood, NJ) at $100\ \text{U/mL}$ in a $0.1\ \text{M}$ Tris-base, $0.25\ \text{M}$ CaCl_2 solution, at pH 7.4, was added to the gels. Gels were incubated with collagenase at $37\ ^\circ\text{C}$ for 4 hours to degrade the collagen. A sandwich ELISA for bFGF was performed on rinse step as well as the collected supernatant samples according to manufacturer's directions (Super-X Elisa, Antigenix, Huntington Station, NY). bFGF in the rinse was used to determine the amount of bFGF remaining in the gels. Quantification of bFGF in the supernatant samples allowed for determination of cumulative release over time, calculated as a percent of the bFGF remaining in the gels after the rinse step. A second experiment was performed by forming gels in the described manner, rinsing, and changing and collecting the supernatant after 24 hours. The gels were then incubated with collagenase for 4 hours and a sample of the supernatant was taken. To release remaining bFGF, $100\ \mu\text{L}$ of a $1.5\ \text{M}$ NaCl solution was added to each tube and incubated for 1 hour. The supernatant was sampled again and a sandwich ELISA for bFGF was run on the supernatant samples according to the manufacturer's directions.

2.6 Infarct and injection surgeries

Female Sprague Dawley rats ($225\text{--}250\ \text{g}$) were given an MI via 25 min occlusion-reperfusion of the left coronary artery using a modified previously published protocol [13]. Briefly, animals were anesthetized under 5% isoflurane and then maintained at 2.5% isoflurane for the remainder the procedure. The rats were placed in a supine position and the chests were cleaned and shaved. Using aseptic technique, the chests were then opened by performing a thoracotomy, accessing the pericardial space and using suture to temporarily occlude the left coronary artery. One week later, all rats received an injection of $75\ \mu\text{L}$ of one of the following groups: bFGF in PPM, bFGF in collagen, bFGF in saline, PPM, collagen, or saline. The injection procedure was performed under isoflurane, following a well described protocol [13, 51]. Briefly, animals were placed in supine position and an incision was made from the xyphoid process along the abdomen. A small incision is made in the diaphragm to access the apex of the heart. $75\ \mu\text{L}$ samples were drawn up into a syringe and injected into the LV-free wall through a 30-gauge needle. Care was taken to prevent puncture of the left ventricle. For each growth factor group, $10\ \mu\text{g}$ of bFGF was used. On day 5 post-injection (day 12 post-infarct), all animals were euthanized. In order to evaluate anastomosis of the vessels formed as a result of the material and growth factor injections, before euthanasia, two animals from each group were perfused with carboxylated red fluorescent microbeads retrograde via the abdominal aorta as previously described [52].

2.7 Histological and immunohistochemical analysis

After sacrifice, hearts were resected, fresh frozen in OCT, and short axis cross sections were taken every 300 μm from apex to base throughout each heart. Sections were fixed with acetone and stained with hematoxylin and eosin (H&E) to identify the infarct region. Infarct screening based on histological (H&E) analysis was done to exclude hearts with small or no infarcts; 2–3 animals were excluded per group prior to any analysis, leaving $n = 6$ –7 remaining for each injection group. The 5 tissue sections in which the infarct region was largest were identified in each heart. These slides were examined by an experienced histopathologist who was blinded to the study groups. The slides were qualitatively scored from 1 to 5 and an average, overall score was assigned to each heart. A score of 1 is defined as a few inflammatory cells or mild inflammation; 2 as mild to moderate inflammation; 3 as moderate inflammation; 4 as moderate to severe inflammation; and 5 as severe inflammation with any necrosis.

Slides from the 5 previously identified sections were co-stained with fluorescein-isothiocyanate-labeled isolectin (1:100) (Vector Labs, Burlingame, CA) to visualize endothelial cells and anti-smooth muscle α -actin (1:50) (Dako, Carpinteria, CA) with an AlexaFluor 488 secondary antibody (1:1000) (Invitrogen, Carlsbad, CA) to visualize smooth muscle cells. Nuclei were visualized with fluorescent Hoescht 33342. Five images were taken evenly spaced throughout the infarct region on each section. Infarct regions were outlined and the arteriole density within the region was quantified. Any vessel that stained positive for anti-SMA and had an average lumen diameter greater than 10 μm was included. Remaining bFGF in the tissue was identified with an anti-human bFGF antibody at a dilution of 1:100 and an AlexaFluor 488 secondary antibody at a dilution of 1:1000. Anastomosis was evaluated within the relevant sections by staining with the anti-SMA antibody with an AlexaFluor 568 secondary antibody at a dilution of 1:200 to visualize the vessels in green and the fluorescent microbeads in red.

2.8 Statistical Analysis

All data is presented as the mean \pm standard error. Statistical significance was calculated by performing a one-way ANOVA followed by a Bonferroni post hoc analysis for all results with multiple groups (data presented in Figures 5 and 7). A student's T-test with a Tukey correction was used to determine statistical significance for the *in vitro* retention experiment (data presented in Figure 4) and the inflammation scores. Statistical significance was accepted when $p < 0.05$.

3. Results

3.1 Confirmation of sulfated GAG content

Sulfated glycosaminoglycans have been previously identified in ECM-derived hydrogels [6–8, 49, 53]; here both FTIR and a Blyscan assay for sGAGs were used to confirm and quantify sGAGs in the porcine pericardial matrix (PPM). The Blyscan assay indicated the PPM retained $26.5 \pm 3.4 \mu\text{g}$ of sGAGs per mg dry ECM, while no sGAGs were present by Blyscan on rat tail collagen I. These values are comparable to those found for matrix hydrogels derived from myocardial and adipose tissue [7, 54]. The FTIR spectrum for the rat tail collagen type I contained characteristic absorption bands at 1649 cm^{-1} (amide I), 1545 cm^{-1} (amide II), and 1339 cm^{-1} (amide III) [55–58]. The FTIR spectrum obtained for PPM (Fig. 1) indicated the presence of sulfate groups as well sugar residues [55]. Peaks in the PPM IR spectrum correlated with the characteristic spectral features of sGAGs, similar to previously published work comparing proteoglycans and collagen in cartilage [55]. Both chondroitin sulfate and heparan sulfate contain absorption bands at 1240 cm^{-1} indicative of S=O stretch of R-SO_3^{-1} and absorption bands characteristic of polysaccharides from 1200–

1000 cm^{-1} (C-C-O and C-O-C stretches). Taken together, the Blyscan assay and FTIR on the PPM confirm the presence of sGAGs.

3.2 Rheometry and SEM

In order to determine that the effects observed *in vitro* and *in vivo* were due to the association of bFGF with the pericardial matrix and not simply a change in diffusion due to a difference in the structural properties, rheometry and SEM were performed on both PPM and collagen gels. The storage moduli for the PPM and collagen gels were 6.5 ± 1.7 Pa and 7.7 ± 0.7 Pa, respectively, values which are not significantly different from each other (Fig. 2). Loss moduli for the PPM and collagen gels were 1.3 ± 0.3 and 0.9 ± 0.2 Pa, respectively. Fiber diameter was analyzed from images taken at 20,000x (Fig. 3) – fibers ranged widely in both materials, most were on the order of hundreds of nanometers, similar to other work with these hydrogels [49, 59]. There were approximately 2.5 ± 0.3 and 2.2 ± 0.2 fibers per linear micron in the PPM and collagen, respectively.

3.3 bFGF retention *in vitro*

To evaluate whether the processed pericardial matrix would retain its native growth factor binding capability, an *in vitro* study was first performed. bFGF was encapsulated in either PPM or collagen gels, and release was determined via ELISA. The incorporated bFGF diffused out of the collagen gels quickly compared to the PPM gels; cumulative release from the collagen gels reached $73.5 \pm 0.62\%$ by the fifth day (prior to treatment with collagenase), while only $27.8 \pm 4.1\%$ of the bFGF was released from the PPM gels (Fig. 4a). After collagenase treatment, the collagen gels were completely degraded and the cumulative release reached $82 \pm 2.9\%$; however, an intact structure remained with the PPM gels and cumulative release only increased to $33 \pm 4.1\%$. To confirm that bFGF was still bound to the remaining components of the PPM gels, a high ionic strength buffer (1.5 M NaCl) was employed, which releases growth factors that bind electrostatically to sulfated sugars [60]. Similar to the previous experiment, gels were rinsed and the supernatant was sampled after 24 hours, followed by sequential incubation with collagenase and NaCl. As expected, the addition of 1.5 M NaCl did not change the cumulative release from collagen gels ($84.5 \pm 6.5\%$ to $85.0 \pm 6.3\%$). The salt did, however, release remaining bFGF from the PPM gels – cumulative release reached $82 \pm 4.1\%$ (Fig. 4b).

3.4 bFGF retention *in vivo*

After first establishing the ability of the ECM-derived hydrogel to enhance growth factor retention *in vitro*, we next explored whether the PPM gel could enhance delivery of bFGF in the setting of myocardial infarction. Here, of the 80 Sprague Dawley rats that received a myocardial infarction, 54 survived the initial surgery and were injected on day 7 post-MI with either PPM, collagen, or saline with or without bFGF ($n = 9$ per group). Upon histological analysis of tissue sections from the hearts, which were resected 5 days post-injection (12 days post-MI), hearts with no infarct, or a small infarct, were excluded from the study and no further analysis was done on that tissue. A total of 16 animals were excluded, after which the sample distribution was as follows: bFGF in PPM, $n = 6$, bFGF in collagen, $n = 7$, bFGF in saline, $n = 6$, PPM, $n = 6$, collagen, $n = 7$, and saline, $n = 6$.

Analysis of the tissue sections obtained after sacrifice five days post-injection indicated increased retention in the bFGF in PPM group compared to bFGF in saline ($p < 0.05$); due to high variability, other differences were not significant, though retention trends upward from delivery in saline to collagen to PPM. Thus, at five days post-injection, a significantly increased amount of bFGF was retained in the tissue when injected in the ECM-derived hydrogel when compared to a bolus injection in saline, with a trend towards increased retention when compared to delivery in collagen.

3.5 Enhanced neovascularization *in vivo*

Beyond establishing the binding and retention of bFGF injected in an ECM-derived hydrogel, the ultimate goal of investigating this growth factor delivery system was to determine if additional activity can be achieved by delivering growth factors through inherent sGAGs in the material. In this case, we assessed the ability of this system to enhance bFGF-mediated neovascularization in ischemic myocardium. Here, acute vascularization was examined 5 days post-injection (12 days post-MI) to determine if the extended retention of bFGF had a significant effect on vessel formation (Fig. 6). Quantification of arteriole density showed that only bFGF in PPM significantly increased arteriole density within the infarct region ($p < 0.05$) when compared to the controls (Fig. 7). Injecting bFGF in PPM resulted in a statistically significant increase in arteriole density (arterioles/mm²) with respect to injecting bFGF in collagen, bFGF in saline, PPM, collagen, or saline. This increase was approximately 112% higher than when bFGF was delivered in collagen. After binning the data into diameter ranges, it was observed that the majority of vessels (70–75%) had average diameters of 10–25 μm ; injecting bFGF in PPM produced a significantly greater number of arterioles both in this range and in the 25–50 μm range compared to the other groups (Fig. 7). The increase in vessels alone is not sufficient to establish increased vascularization of the infarct region – the vessels must be perfused and delivering blood to the damaged region. We therefore confirmed the existence of anastomosed neovasculature by the presence of perfused microbeads within the arterioles formed in the infarct region. Presence of microbeads indicated that vessels formed through the delivery of bFGF in PPM were in fact functional (Fig. 8).

In order to assess the potential influence of inflammation on our neovascularization results, we performed a semi-quantitative assessment of tissue sections from each group. The result of a blinded pathologist's score of the tissue indicated that injection of growth factor in any form – alone, with collagen, or with pericardial matrix – caused an increase in the inflammation score (from mild/moderate to moderate/severe) that was statistically significant compared to the saline-injected hearts ($p < 0.05$). Injection of the materials alone showed a trend toward increased inflammation (from mild/moderate to moderate), but the degree was not statistically significant compared to the saline-injected hearts or to each other.

4. Discussion

Growth factor delivery systems have been designed from a variety of materials – both inert and bioactive. These systems are diverse and numerous, taking the form of injectable microspheres [61], implantable patches [38, 62], and *in situ* gelling scaffolds [3, 4, 63]. *In vivo*, growth factor delivery is achieved via sequestration in the native extracellular matrix. Through binding to sulfated glycosaminoglycans linked to ECM proteins, growth factors can be immobilized for presentation or stored for future release [64]. When designing tissue engineering approaches that mimic this system, important design parameters include providing for prolonged presentation and release of the incorporated growth factors, as well as a fibrous, porous template that allows for cellular infiltration and remodeling. A wide array of materials have previously been investigated for encapsulation of angiogenic factors for therapeutic delivery [29], including synthetic materials such as poly(lactide-co-glycolide) (PLG) [65] and poly-NiPAam co-polymers [66], as well as natural materials such as alginate [67, 68], fibrin [26, 69], collagen [70], gelatin [71], and chitosan [72–74], among others. Often, a material that has been demonstrated to be a useful scaffold for a certain tissue engineering application will be modified to deliver growth factors in order to enhance the therapeutic effect. Common modifications include crosslinking the material or covalently attaching growth factors [38, 62] or growth factor-binding molecules such as heparin [75]. Previous work has shown that when angiogenic growth factors are

immobilized on a scaffold, angiogenic potential is enhanced [37, 76]. Unfortunately, the modifications used to increase growth factor activity or stability may change the chemistry of many natural biopolymers and therefore change their activity *in vivo* [46]. ECM-derived hydrogels processed from decellularized tissue have shown great promise as scaffolds for tissue repair, but their potential as growth factor delivery systems had not been previously explored. These matrix hydrogels have been demonstrated to retain components of the native ECM, including proteins, glycoproteins, and glycosaminoglycans [6–8, 49, 53]; implying the possibility of employing the same method for sequestration and delivery observed in the native tissue microenvironment. With this work, the natural incorporation of a heparin binding growth factor, bFGF, in a pericardial matrix hydrogel was explored.

Confirmation of the sulfated GAG content in the PPM gel was performed by comparing the FTIR spectra obtained for PPM and collagen and identifying a sulfate peak and a sugar peak (Fig. 1), similar to previous work comparing proteoglycans and collagen in cartilage [55]. A Blyscan sulfated glycosaminoglycan assay allowed for quantification of the sGAG content, which was comparable to matrix hydrogels derived from myocardial and adipose tissue [7, 54]. While bFGF diffused readily out of the collagen gels over 5 days *in vitro*, significant release of bFGF from the PPM gels was only observed after the addition of NaCl (Fig. 4b), indicating that the growth factor was bound to the matrix through electrostatic means, presumably through the sGAGs in the material. A portion of bFGF did diffuse out of the PPM gel over 5 days, indicating that some of the growth factor was simply encapsulated in the material instead of bound. Upon the addition of collagenase, additional bFGF was removed as the collagen structure was degraded; however, the remaining components of the gel, which were visible in an intact 3D structure, retained a significant amount of growth factor that was dissociated upon the further addition of NaCl. These *in vitro* results with enhanced retention were further validated by the increased retention *in vivo*, quantified five days post-injection (Fig. 5d). This data, taken in conjunction with the similar mechanical and structural properties of the two materials, indicates that the growth factors are likely associating with the extant binding domains in the decellularized ECM hydrogel.

Using biomaterials for immobilization and prolonged release of angiogenic factors has been shown to enhance their activity; in this study, injection of bFGF in pericardial matrix was the only treatment group to significantly increase acute neovascularization compared to controls (Fig. 7). Additionally, a significantly greater density of large-diameter vessels (25–50 μm) were identified in the infarcts in these animals (Fig. 7), indicating a maturation of the vasculature. These results may be due to the extended presence of bFGF in the injected PPM or an increase in stability or activity due to immobilization on the PPM scaffold. There may also be synergistic effects with the addition of bFGF to the matrix hydrogel. Inflammation is known to influence neovascularization, and the inclusion of bFGF [77, 78] and GAGs [79] as well as differences between allogeneic and xenogeneic material sources could influence this process. We therefore obtained a semi-quantitative score of the inflammation in each group. While an increase in the degree of inflammation was observed with injection of all groups with a growth factor (bFGF alone, bFGF in collagen, and bFGF in pericardial matrix) when compared to the saline injection, there was no significant difference in the inflammatory response of either material alone (pericardial matrix or collagen) when compared to saline or each other. Thus, while an increase in inflammation may be one of the mechanisms by which angiogenesis is enhanced [80], since the inflammatory response was not significantly different among the growth factor groups, it is likely not the major contributing factor in the increased arteriole density observed when bFGF is delivered with the pericardial matrix.

It is important to note that while other studies have shown extant growth factor content (bFGF and VEGF) in decellularized matrix materials after processing, the quantity is on the

order of picograms per milligram of dry weight ECM [81]. While we previously did not identify bFGF in the PPM using mass spectrometry [8], any potential extant bFGF content should be masked by the much larger quantity added to the injection. Additionally, the control pericardial matrix injection did not show a significant increase in arteriole density compared to collagen or saline, indicating the material alone does not enhance neovascularization over other injections at this time point.

Given the potential for hemangioma formation [82–84], where vascular tissue proliferates without being connected to the host vasculature, it was important to determine if using the pericardial matrix hydrogel to deliver bFGF would result in anastomosis of the blood vessels formed in the infarct region. This was done by perfusing red fluorescent carboxylated microspheres retrograde before euthanasia. Red fluorescence in the vessels formed in the infarct region for all bFGF groups indicated that the vessels were connected to the host vasculature (Fig. 8), supporting the feasibility of the pericardial matrix as a delivery system for bFGF. Importantly, even though the high concentration of bFGF injected did not cause hemangioma formation, it would still be necessary to optimize the loading dose of growth factor for any application. In previous studies utilizing bFGF for treatment post-MI, the administered dose varied greatly, from 30 mg injected with 3 mg of heparin sulfate in a canine model [85], 110 mg daily intracoronary bolus injection also in a canine model [86], or a total of 5 ug incorporated in heparin-sepharose-alginate beads in a porcine model [61]. Further investigation with ECM-derived hydrogels will be necessary to determine the maximum loading capacity for a heparin-binding growth factor. This value will vary for matrix hydrogels derived via different methods and from different tissues as it will depend on the concentrations of growth factor-binding motifs in the processed materials.

Injectable matrix hydrogels derived from different tissue sources have been previously explored as therapies for the prevention of heart failure post-myocardial infarction [11]. Intramyocardial injection of hydrogels derived from porcine myocardium and small-intestinal submucosa has been demonstrated to preserve ejection fraction post-MI while saline-injected control animals continue to decline [13, 14]. While the exact mechanism behind this success has not yet been elucidated, it may be that the fibrous microstructure provides a template for cell infiltration and vascularization [87–89] or that degradation may promote cell in-growth and tissue remodeling [11, 90]. ECM-derived hydrogels are of special clinical interest as they are deliverable via catheter and therefore could potentially be administered via minimally invasive methods [13]. While long-term studies with this growth factor delivery system will be necessary to evaluate its effect on cardiac function and remodeling post-MI, with this work, we have established proof-of-concept for using an ECM-derived hydrogel to enhance retention and delivery of a heparin-binding growth factor.

5. Conclusions

Thus, with this work we have demonstrated, both *in vitro* and *in vivo*, that the porcine pericardial matrix hydrogel, with its sulfated sugars, has the ability to sequester bFGF. By relying on the sGAG component of the ECM-derived hydrogel to bind bFGF, the angiogenic growth factor was bound and presented in a manner similar to growth factors in the native ECM. In a rodent MI model, intramyocardial injection of bFGF in PPM was the only group to demonstrate enhanced acute neovascularization post-MI when compared to controls. We have demonstrated the potential use of a decellularized ECM-derived hydrogel as a growth factor delivery system for tissue engineering applications. While bFGF was used as the model growth factor in this study, other heparin-binding growth factors could be incorporated in a similar fashion. Additionally, the findings of this study imply that the sulfated GAG content in other ECM-derived hydrogels would provide a platform for the

incorporation of heparin-binding growth factors. This incorporation can be achieved without additional chemical modification and could allow for prolonged delivery of the growth factors to the site of application.

Acknowledgments

The authors would like to thank Todd Johnson, Samantha Evans, and Anthony Monteforte for their help in tissue preparation and sectioning as well as Greg Grover, Andrea Potocny, and the Sailor Lab for assistance with FTIR. This research was supported in part by the NIH Director's New Innovator Award Program, part of the NIH Roadmap for Medical Research, through grant number 1-DP2-OD004309-01. S.B.S.-N. would like to thank the NSF for a Graduate Research Fellowship.

References

1. Patel ZS, Mikos AG. Angiogenesis with biomaterial-based drug- and cell-delivery systems. *J Biomater Sci Polym Ed.* 2004; 15:701–726. [PubMed: 15255521]
2. Drury JL, Mooney DJ. Hydrogels for tissue engineering: scaffold design variables and applications. *Biomaterials.* 2003; 24:4337–4351. [PubMed: 12922147]
3. Dai W, Wold LE, Dow JS, Kloner RA. Thickening of the infarcted wall by collagen injection improves left ventricular function in rats: a novel approach to preserve cardiac function after myocardial infarction. *J Am Coll Cardiol.* 2005; 46:714–719. [PubMed: 16098441]
4. Landa N, Miller L, Feinberg MS, Holbova R, Shachar M, Freeman I, Cohen S, Leor J. Effect of injectable alginate implant on cardiac remodeling and function after recent and old infarcts in rat. *Circulation.* 2008; 117:1388–1396. [PubMed: 18316487]
5. Fujimoto KL, Ma Z, Nelson DM, Hashizume R, Guan J, Tobita K, Wagner WR. Synthesis, characterization and therapeutic efficacy of a biodegradable, thermoresponsive hydrogel designed for application in chronic infarcted myocardium. *Biomaterials.* 2009; 30:4357–4368. [PubMed: 19487021]
6. Young DA, Ibrahim DO, Hu D, Christman KL. Injectable hydrogel scaffold from decellularized human lipoaspirate. *Acta Biomater.* 2011; 7:1040–1049. [PubMed: 20932943]
7. Singelyn JM, DeQuach JA, Seif-Naraghi SB, Littlefield RB, Schup-Magoffin PJ, Christman KL. Naturally derived myocardial matrix as an injectable scaffold for cardiac tissue engineering. *Biomaterials.* 2009; 30:5409–5416. [PubMed: 19608268]
8. Seif-Naraghi SB, Salvatore MA, Schup-Magoffin PJ, Hu DP, Christman KL. Design and characterization of an injectable pericardial matrix gel: a potentially autologous scaffold for cardiac tissue engineering. *Tissue engineering Part A.* 2010; 16:2017–2027. [PubMed: 20100033]
9. Freytes DO, Martin J, Velankar SS, Lee AS, Badylak SF. Preparation and rheological characterization of a gel form of the porcine urinary bladder matrix. *Biomaterials.* 2008; 29:1630–1637. [PubMed: 18201760]
10. Crapo PM, Gilbert TW, Badylak SF. An overview of tissue and whole organ decellularization processes. *Biomaterials.* 32:3233–3243. [PubMed: 21296410]
11. Singelyn JM, Christman KL. Injectable materials for the treatment of myocardial infarction and heart failure: the promise of decellularized matrices. *J Cardiovasc Transl Res.* 3:478–486. [PubMed: 20632221]
12. Gilbert TW, Sellaro TL, Badylak SF. Decellularization of tissues and organs. *Biomaterials.* 2006; 27:3675–3683. [PubMed: 16519932]
13. Singelyn JM, Sundaramurthy P, Johnson TD, Schup-Magoffin PJ, Hu DP, Faulk DM, Wang J, Mayle KM, Bartels K, Salvatore M, Kinsey AM, DeMaria AN, Dib N, Christman KL. Catheter-Deliverable Hydrogel Derived From Decellularized Ventricular Extracellular Matrix Increases Endogenous Cardiomyocytes and Preserves Cardiac Function Post-Myocardial Infarction. *J Am Coll Cardiol.* 2012; 59:751–763. [PubMed: 22340268]
14. Okada M, Payne TR, Oshima H, Momoi N, Tobita K, Huard J. Differential efficacy of gels derived from small intestinal submucosa as an injectable biomaterial for myocardial infarct repair. *Biomaterials.* 2010; 31:7678–7683. [PubMed: 20674011]

15. Emanuelli C, Salis MB, Stacca T, Gaspa L, Chao J, Chao L, Piana A, Madeddu P. Rescue of impaired angiogenesis in spontaneously hypertensive rats by intramuscular human tissue kallikrein gene transfer. *Hypertension*. 2001; 38:136–141. [PubMed: 11463774]
16. Carmeliet P, Conway EM. Growing better blood vessels. *Nat Biotechnol*. 2001; 19:1019–1020. [PubMed: 11689842]
17. Asahara T, Bauters C, Zheng LP, Takeshita S, Bunting S, Ferrara N, Symes JF, Isner JM. Synergistic effect of vascular endothelial growth factor and basic fibroblast growth factor on angiogenesis in vivo. *Circulation*. 1995; 92:II365–371. [PubMed: 7586439]
18. Isner JM, Asahara T. Angiogenesis and vasculogenesis as therapeutic strategies for postnatal neovascularization. *J Clin Invest*. 1999; 103:1231–1236. [PubMed: 10225965]
19. Laham RJ, Sellke FW, Edelman ER, Pearlman JD, Ware JA, Brown DL, Gold JP, Simons M. Local perivascular delivery of basic fibroblast growth factor in patients undergoing coronary bypass surgery: results of a phase I randomized, double-blind, placebo-controlled trial. *Circulation*. 1999; 100:1865–1871. [PubMed: 10545430]
20. Kellar RS, Landeen LK, Shepherd BR, Naughton GK, Ratcliffe A, Williams SK. Scaffold-based three-dimensional human fibroblast culture provides a structural matrix that supports angiogenesis in infarcted heart tissue. *Circulation*. 2001; 104:2063–2068. [PubMed: 11673347]
21. West DC, Hampson IN, Arnold F, Kumar S. Angiogenesis induced by degradation products of hyaluronic acid. *Science*. 1985; 228:1324–1326. [PubMed: 2408340]
22. Fournier N, Doillon CJ. Biological molecule-impregnated polyester: an in vivo angiogenesis study. *Biomaterials*. 1996; 17:1659–1665. [PubMed: 8866027]
23. Hung WS, Fang CL, Su CH, Lai WF, Chang YC, Tsai YH. Cytotoxicity and immunogenicity of SACCHACHITIN and its mechanism of action on skin wound healing. *J Biomed Mater Res*. 2001; 56:93–100. [PubMed: 11309795]
24. Binzen E, Rickert D, Kelch S, Fuhrmann R. Angiogenesis around new AB-polymer networks after one week of implantation in mice. *Clin Hemorheol Microcirc*. 2003; 28:183–188. [PubMed: 12775900]
25. Pandit AS, Feldman DS, Caulfield J. In vivo wound healing response to a modified degradable fibrin scaffold. *J Biomater Appl*. 1998; 12:222–236. [PubMed: 9493069]
26. Pandit AS, Feldman DS, Caulfield J, Thompson A. Stimulation of angiogenesis by FGF-1 delivered through a modified fibrin scaffold. *Growth Factors*. 1998; 15:113–123. [PubMed: 9505167]
27. Goncalves LM. Angiogenic growth factors: potential new treatment for acute myocardial infarction? *Cardiovasc Res*. 2000; 45:294–302. [PubMed: 10728349]
28. Soker S, Machado M, Atala A. Systems for therapeutic angiogenesis in tissue engineering. *World J Urol*. 2000; 18:10–18. [PubMed: 10766038]
29. Zisch AH, Lutolf MP, Hubbell JA. Biopolymeric delivery matrices for angiogenic growth factors. *Cardiovasc Pathol*. 2003; 12:295–310. [PubMed: 14630296]
30. Lei Y, Haider H, Shujia J, Sim ES. Therapeutic angiogenesis. Devising new strategies based on past experiences. *Basic Res Cardiol*. 2004; 99:121–132. [PubMed: 14963670]
31. Henry TD, Annex BH, McKendall GR, Azrin MA, Lopez JJ, Giordano FJ, Shah PK, Willerson JT, Benza RL, Berman DS, Gibson CM, Bajamonde A, Rundle AC, Fine J, McCluskey ER. The VIVA trial: Vascular endothelial growth factor in Ischemia for Vascular Angiogenesis. *Circulation*. 2003; 107:1359–1365. [PubMed: 12642354]
32. Haider H, Ye L, Jiang S, Ge R, Law PK, Chua T, Wong P, Sim EK. Angiomyogenesis for cardiac repair using human myoblasts as carriers of human vascular endothelial growth factor. *J Mol Med*. 2004; 82:539–549. [PubMed: 15175859]
33. Mann BK, Schmedlen RH, West JL. Tethered-TGF-beta increases extracellular matrix production of vascular smooth muscle cells. *Biomaterials*. 2001; 22:439–444. [PubMed: 11214754]
34. Tayalia P, Mooney DJ. Controlled growth factor delivery for tissue engineering. *Adv Mater*. 2009; 21:3269–3285. [PubMed: 20882497]
35. Lee KY, Peters MC, Anderson KW, Mooney DJ. Controlled growth factor release from synthetic extracellular matrices. *Nature*. 2000; 408:998–1000. [PubMed: 11140690]

36. Chen RR, Mooney DJ. Polymeric growth factor delivery strategies for tissue engineering. *Pharm Res.* 2003; 20:1103–1112. [PubMed: 12948005]
37. Shen YH, Shoichet MS, Radisic M. Vascular endothelial growth factor immobilized in collagen scaffold promotes penetration and proliferation of endothelial cells. *Acta Biomater.* 2008; 4:477–489. [PubMed: 18328795]
38. Miyagi Y, Chiu LL, Cimini M, Weisel RD, Radisic M, Li RK. Biodegradable collagen patch with covalently immobilized VEGF for myocardial repair. *Biomaterials.* 2011; 32:1280–1290. [PubMed: 21035179]
39. Kim JH, Jung Y, Kim SH, Sun K, Choi J, Kim HC, Park Y. The enhancement of mature vessel formation and cardiac function in infarcted hearts using dual growth factor delivery with self-assembling peptides. *Biomaterials.* 32:6080–6088. [PubMed: 21636123]
40. Sakiyama-Elbert SE, Hubbell JA. Controlled release of nerve growth factor from a heparin-containing fibrin-based cell ingrowth matrix. *J Control Release.* 2000; 69:149–158. [PubMed: 11018553]
41. Pieper JS, Hafmans T, van Wachem PB, van Luyn MJ, Brouwer LA, Veerkamp JH, van Kuppevelt TH. Loading of collagen-heparan sulfate matrices with bFGF promotes angiogenesis and tissue generation in rats. *J Biomed Mater Res.* 2002; 62:185–194. [PubMed: 12209938]
42. Freeman I, Kedem A, Cohen S. The effect of sulfation of alginate hydrogels on the specific binding and controlled release of heparin-binding proteins. *Biomaterials.* 2008; 29:3260–3268. [PubMed: 18462788]
43. Sakiyama SE, Schense JC, Hubbell JA. Incorporation of heparin-binding peptides into fibrin gels enhances neurite extension: an example of designer matrices in tissue engineering. *Faseb J.* 1999; 13:2214–2224. [PubMed: 10593869]
44. Sakiyama-Elbert SE, Hubbell JA. Development of fibrin derivatives for controlled release of heparin-binding growth factors. *J Control Release.* 2000; 65:389–402. [PubMed: 10699297]
45. Miyagi Y, Chiu LL, Cimini M, Weisel RD, Radisic M, Li RK. Biodegradable collagen patch with covalently immobilized VEGF for myocardial repair. *Biomaterials.* 32:1280–1290. [PubMed: 21035179]
46. Berger J, Reist M, Mayer JM, Felt O, Peppas NA, Gurny R. Structure and interactions in covalently and ionically crosslinked chitosan hydrogels for biomedical applications. *Eur J Pharm Biopharm.* 2004; 57:19–34. [PubMed: 14729078]
47. Iozzo, RV. *Proteoglycans: structure, biology, and molecular interactions.* New York: Marcel Dekker; 2000.
48. Mirsadraee S, Wilcox HE, Korossis SA, Kearney JN, Watterson KG, Fisher J, Ingham E. Development and characterization of an acellular human pericardial matrix for tissue engineering. *Tissue Eng.* 2006; 12:763–773. [PubMed: 16674290]
49. Seif-Naraghi SB, Horn D, Schup-Magoffin PA, Madani MM, Christman KL. Patient-to-Patient Variability in Autologous Pericardial Matrix Scaffolds for Cardiac Repair. *J Cardiovasc Transl Res.* 2011
50. Johnston N, Dettmar PW, Bishwokarma B, Lively MO, Koufman JA. Activity/stability of human pepsin: implications for reflux attributed laryngeal disease. *Laryngoscope.* 2007; 117:1036–1039. [PubMed: 17417109]
51. Christman KL, Fok HH, Sievers RE, Fang Q, Lee RJ. Fibrin glue alone and skeletal myoblasts in a fibrin scaffold preserve cardiac function after myocardial infarction. *Tissue Eng.* 2004; 10:403–409. [PubMed: 15165457]
52. Christman KL, Fang Q, Yee MS, Johnson KR, Sievers RE, Lee RJ. Enhanced neovasculature formation in ischemic myocardium following delivery of pleiotrophin plasmid in a biopolymer. *Biomaterials.* 2005; 26:1139–1144. [PubMed: 15451633]
53. Hodde JP, Badylak SF, Brightman AO, Voytik-Harbin SL. Glycosaminoglycan content of small intestinal submucosa: a bioscaffold for tissue replacement. *Tissue Eng.* 1996; 2:209–217. [PubMed: 19877943]
54. Young DA, Ibrahim DO, Hu D, Christman KL. Injectable hydrogel scaffold from decellularized human lipoaspirate. *Acta Biomater.* 7:1040–1049. [PubMed: 20932943]

55. Camacho NP, West P, Torzilli PA, Mendelsohn R. FTIR microscopic imaging of collagen and proteoglycan in bovine cartilage. *Biopolymers*. 2001; 62:1–8. [PubMed: 11135186]
56. Huc A, Sanejouand J. [Study of the infra-red spectrum of acid-soluble collagen]. *Biochimica et biophysica acta*. 1968; 154:408–410. [PubMed: 5637059]
57. Lazarev YA, Grishkovsky BA, Khromova TB. Amide I band of IR spectrum and structure of collagen and related polypeptides. *Biopolymers*. 1985; 24:1449–1478. [PubMed: 4041546]
58. Potter K, Kidder LH, Levin IW, Lewis EN, Spencer RG. Imaging of collagen and proteoglycan in cartilage sections using Fourier transform infrared spectral imaging. *Arthritis and rheumatism*. 2001; 44:846–855. [PubMed: 11315924]
59. Johnson TD, Lin SY, Christman KL. Tailoring material properties of a nanofibrous extracellular matrix derived hydrogel. *Nanotechnology*. 2011; 22:494015. [PubMed: 22101810]
60. Capila I, Linhardt RJ. Heparin-protein interactions. *Angew Chem Int Ed Engl*. 2002; 41:391–412. [PubMed: 12491369]
61. Harada K, Grossman W, Friedman M, Edelman ER, Prasad PV, Keighley CS, Manning WJ, Sellke FW, Simons M. Basic fibroblast growth factor improves myocardial function in chronically ischemic porcine hearts. *J Clin Invest*. 1994; 94:623–630. [PubMed: 7518840]
62. Shen YH, Shoichet MS, Radisic M. Vascular endothelial growth factor immobilized in collagen scaffold promotes penetration and proliferation of endothelial cells. *Acta Biomater*. 2008; 4:477–489. [PubMed: 18328795]
63. Christman KL, Vardanian AJ, Fang Q, Sievers RE, Fok HH, Lee RJ. Injectable fibrin scaffold improves cell transplant survival, reduces infarct expansion, and induces neovasculture formation in ischemic myocardium. *Journal of the American College of Cardiology*. 2004; 44:654–660. [PubMed: 15358036]
64. Patel ZS, Mikos AG. Angiogenesis with biomaterial-based drug- and cell-delivery systems. *J Biomater Sci Polym Ed*. 2004; 15:701–726. [PubMed: 15255521]
65. Richardson TP, Peters MC, Ennett AB, Mooney DJ. Polymeric system for dual growth factor delivery. *Nat Biotechnol*. 2001; 19:1029–1034. [PubMed: 11689847]
66. Garbern JC, Minami E, Stayton PS, Murry CE. Delivery of basic fibroblast growth factor with a pH-responsive, injectable hydrogel to improve angiogenesis in infarcted myocardium. *Biomaterials*. 32:2407–2416. [PubMed: 21186056]
67. Peters MC, Isenberg BC, Rowley JA, Mooney DJ. Release from alginate enhances the biological activity of vascular endothelial growth factor. *J Biomater Sci Polym Ed*. 1998; 9:1267–1278. [PubMed: 9860169]
68. Perets A, Baruch Y, Weisbuch F, Shoshany G, Neufeld G, Cohen S. Enhancing the vascularization of three-dimensional porous alginate scaffolds by incorporating controlled release basic fibroblast growth factor microspheres. *J Biomed Mater Res A*. 2003; 65:489–497. [PubMed: 12761840]
69. Fasol R, Schumacher B, Schlaudraff K, Hauenstein KH, Seitelberger R. Experimental use of a modified fibrin glue to induce site-directed angiogenesis from the aorta to the heart. *J Thorac Cardiovasc Surg*. 1994; 107:1432–1439. [PubMed: 7515132]
70. Fujisato T, Sajiki T, Liu Q, Ikada Y. Effect of basic fibroblast growth factor on cartilage regeneration in chondrocyte-seeded collagen sponge scaffold. *Biomaterials*. 1996; 17:155–162. [PubMed: 8624392]
71. Ikada Y, Tabata Y. Protein release from gelatin matrices. *Adv Drug Deliv Rev*. 1998; 31:287–301. [PubMed: 10837630]
72. Kim SE, Park JH, Cho YW, Chung H, Jeong SY, Lee EB, Kwon IC. Porous chitosan scaffold containing microspheres loaded with transforming growth factor-beta1: implications for cartilage tissue engineering. *J Control Release*. 2003; 91:365–374. [PubMed: 12932714]
73. des Rieux A, Ucakar B, Mupendwa BP, Colau D, Feron O, Carmeliet P, Preat V. 3D systems delivering VEGF to promote angiogenesis for tissue engineering. *J Control Release*. 2011; 150:272–278. [PubMed: 21130820]
74. Chiu LL, Radisic M. Controlled release of thymosin beta4 using collagen-chitosan composite hydrogels promotes epicardial cell migration and angiogenesis. *J Control Release*. 2011

75. Pieper JS, Hafmans T, van Wachem PB, van Luyn MJ, Brouwer LA, Veerkamp JH, van Kuppevelt TH. Loading of collagen-heparan sulfate matrices with bFGF promotes angiogenesis and tissue generation in rats. *J Biomed Mater Res.* 2002; 62:185–194. [PubMed: 12209938]
76. Steffens GC, Yao C, Prevel P, Markowicz M, Schenck P, Noah EM, Pallua N. Modulation of angiogenic potential of collagen matrices by covalent incorporation of heparin and loading with vascular endothelial growth factor. *Tissue Eng.* 2004; 10:1502–1509. [PubMed: 15588409]
77. Zittermann SI, Issekutz AC. Basic fibroblast growth factor (bFGF, FGF-2) potentiates leukocyte recruitment to inflammation by enhancing endothelial adhesion molecule expression. *Am J Pathol.* 2006; 168:835–846. [PubMed: 16507899]
78. Zittermann SI, Issekutz AC. Endothelial growth factors VEGF and bFGF differentially enhance monocyte and neutrophil recruitment to inflammation. *J Leukoc Biol.* 2006; 80:247–257. [PubMed: 16818728]
79. Taylor KR, Gallo RL. Glycosaminoglycans and their proteoglycans: host-associated molecular patterns for initiation and modulation of inflammation. *Faseb J.* 2006; 20:9–22. [PubMed: 16394262]
80. Costa C, Incio J, Soares R. Angiogenesis and chronic inflammation: cause or consequence? *Angiogenesis.* 2007; 10:149–166. [PubMed: 17457680]
81. Hodde JP, Record RD, Liang HA, Badylak SF. Vascular endothelial growth factor in porcine-derived extracellular matrix. *Endothelium.* 2001; 8:11–24. [PubMed: 11409848]
82. Schwarz ER, Speakman MT, Patterson M, Hale SS, Isner JM, Kedes LH, Kloner RA. Evaluation of the effects of intramyocardial injection of DNA expressing vascular endothelial growth factor (VEGF) in a myocardial infarction model in the rat—angiogenesis and angioma formation. *J Am Coll Cardiol.* 2000; 35:1323–1330. [PubMed: 10758976]
83. Ribatti D, Gualandris A, Belleri M, Massardi L, Nico B, Rusnati M, Dell’Era P, Vacca A, Roncali L, Presta M. Alterations of blood vessel development by endothelial cells overexpressing fibroblast growth factor-2. *J Pathol.* 1999; 189:590–599. [PubMed: 10629563]
84. Brown LF, Tognazzi K, Dvorak HF, Hristi TJ. Strong expression of kinase insert domain-containing receptor, a vascular permeability factor/vascular endothelial growth factor receptor in AIDS-associated Kaposi’s sarcoma and cutaneous angiosarcoma. *Am J Pathol.* 1996; 148:1065–1074. [PubMed: 8644848]
85. Uchida Y, Yanagisawa-Miwa A, Nakamura F, Yamada K, Tomaru T, Kimura K, Morita T. Angiogenic therapy of acute myocardial infarction by intrapericardial injection of basic fibroblast growth factor and heparin sulfate: an experimental study. *Am Heart J.* 1995; 130:1182–1188. [PubMed: 7484767]
86. Yanagisawa-Miwa A, Uchida Y, Nakamura F, Tomaru T, Kido H, Kamijo T, Sugimoto T, Kaji K, Utsuyama M, Kurashima C, et al. Salvage of infarcted myocardium by angiogenic action of basic fibroblast growth factor. *Science.* 1992; 257:1401–1403. [PubMed: 1382313]
87. Langer R, Vacanti JP. Tissue engineering. *Science.* 1993; 260:920–926. [PubMed: 8493529]
88. Martina M, Subramanyam G, Weaver JC, Hutmacher DW, Morse DE, Valiyaveetil S. Developing macroporous bicontinuous materials as scaffolds for tissue engineering. *Biomaterials.* 2005; 26:5609–5616. [PubMed: 15878365]
89. Ifkovits JL, Wu K, Mauck RL, Burdick JA. The influence of fibrous elastomer structure and porosity on matrix organization. *PLoS One.* 5:e15717. [PubMed: 21203510]
90. Davis ME, Hsieh PC, Grodzinsky AJ, Lee RT. Custom design of the cardiac microenvironment with biomaterials. *Circ Res.* 2005; 97:8–15. [PubMed: 16002755]

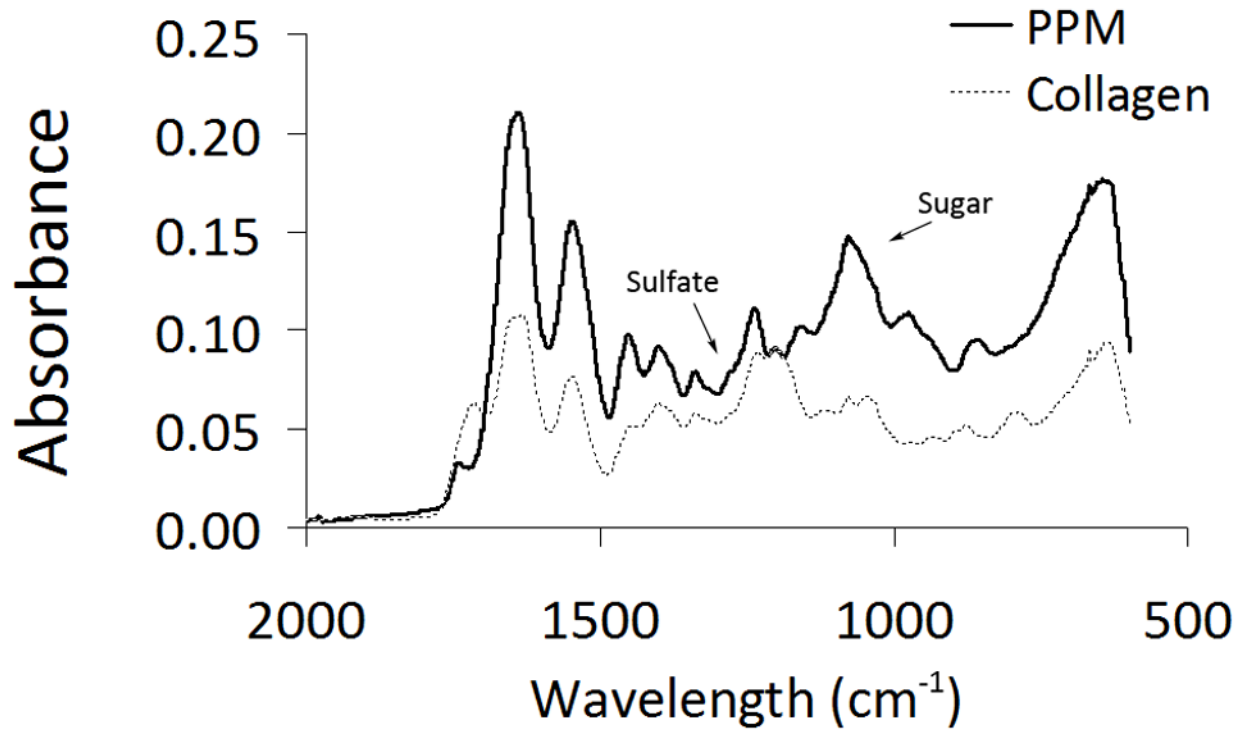


Figure 1. FTIR. Spectra obtained for porcine pericardial matrix and rat tail collagen, both lyophilized after pepsin digestion. Arrows denote carbohydrate peak and sulfate peak.

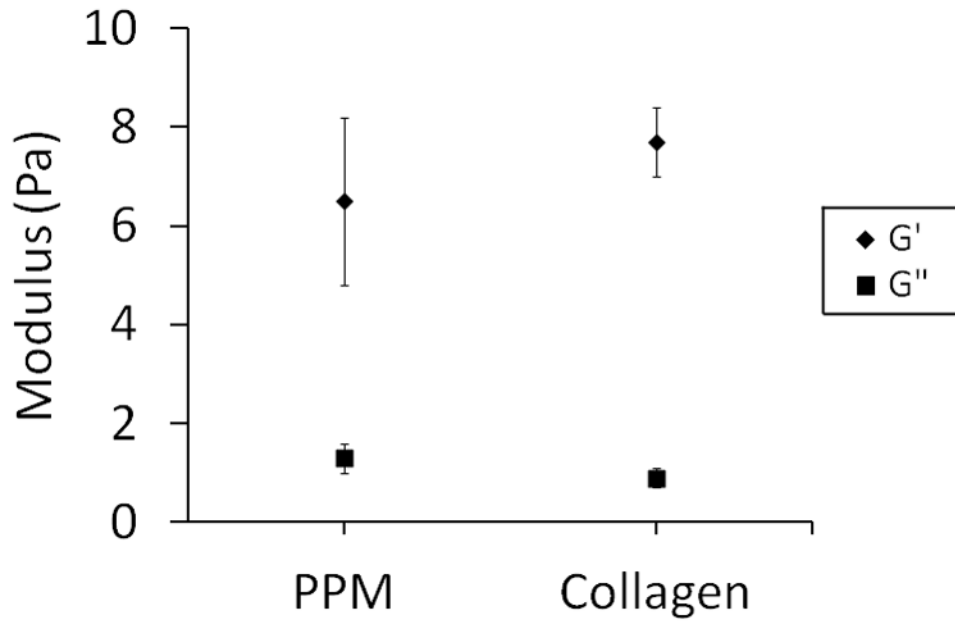


Figure 2. Rheometry. Storage and loss moduli reported at a frequency of 1 rad/s. The two materials are not statistically different, though there is more variability within the pericardial matrix.

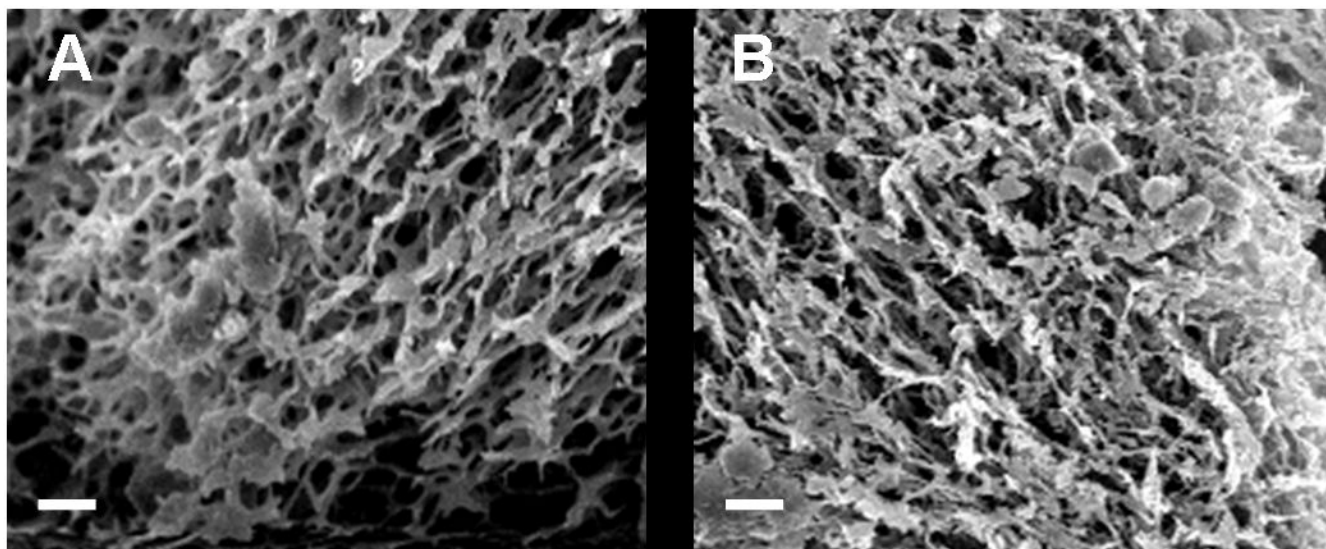


Figure 3. Scanning electron microscopy. Representative images of the microstructure of gels composed of (A) PPM at 6 mg/mL and (B) collagen at 2.5 mg/mL. Fiber diameter and density were similar between the two materials. Scale bar is 2 μ m.

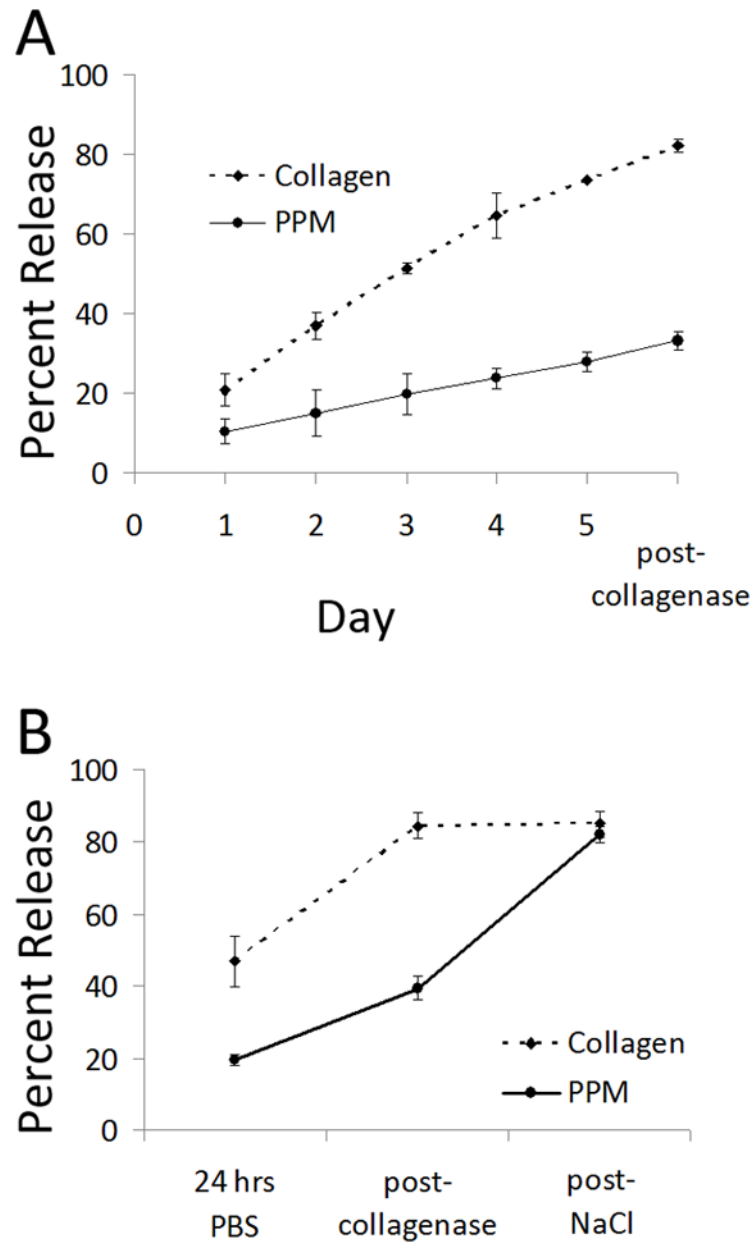


Figure 4. *in vitro* binding and release. (A) Cumulative release of bFGF from porcine pericardial matrix and collagen gels *in vitro* over 5 days, followed by a 4-hour collagenase incubation. (B) Release with 1.5 M NaCl; cumulative release of bFGF from porcine pericardial matrix and collagen gels. Here, incubation with 1.5 M NaCl allowed for release of bFGF from pericardial matrix gels. * $p < 0.05$ compared to PPM at the same timepoint.

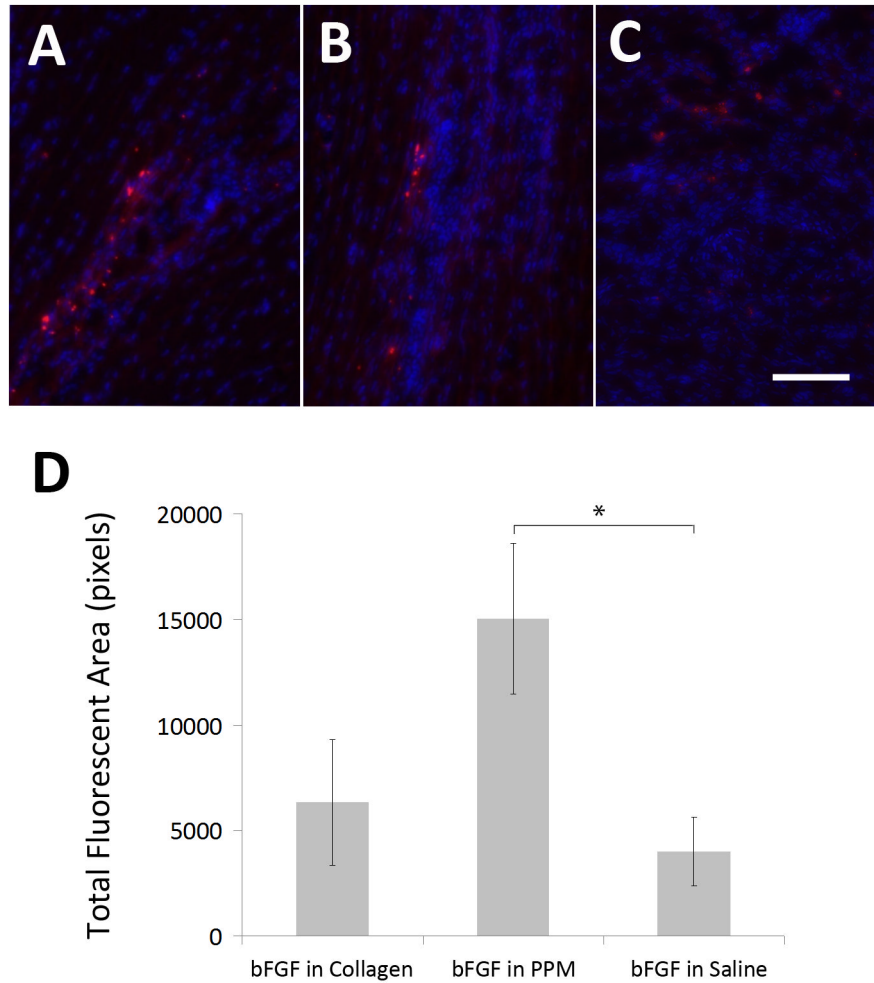


Figure 5. *in vivo* retention. Visualization of bFGF (red) retention in the infarct region in animals injected with bFGF in PPM (A), bFGF in collagen (B), and bFGF in saline (C) *in vivo* after 5 days. Quantification of bFGF in the three groups (D) via total fluorescent area (n = 6–7). Scale bar is 25 μm . * $p < 0.05$.

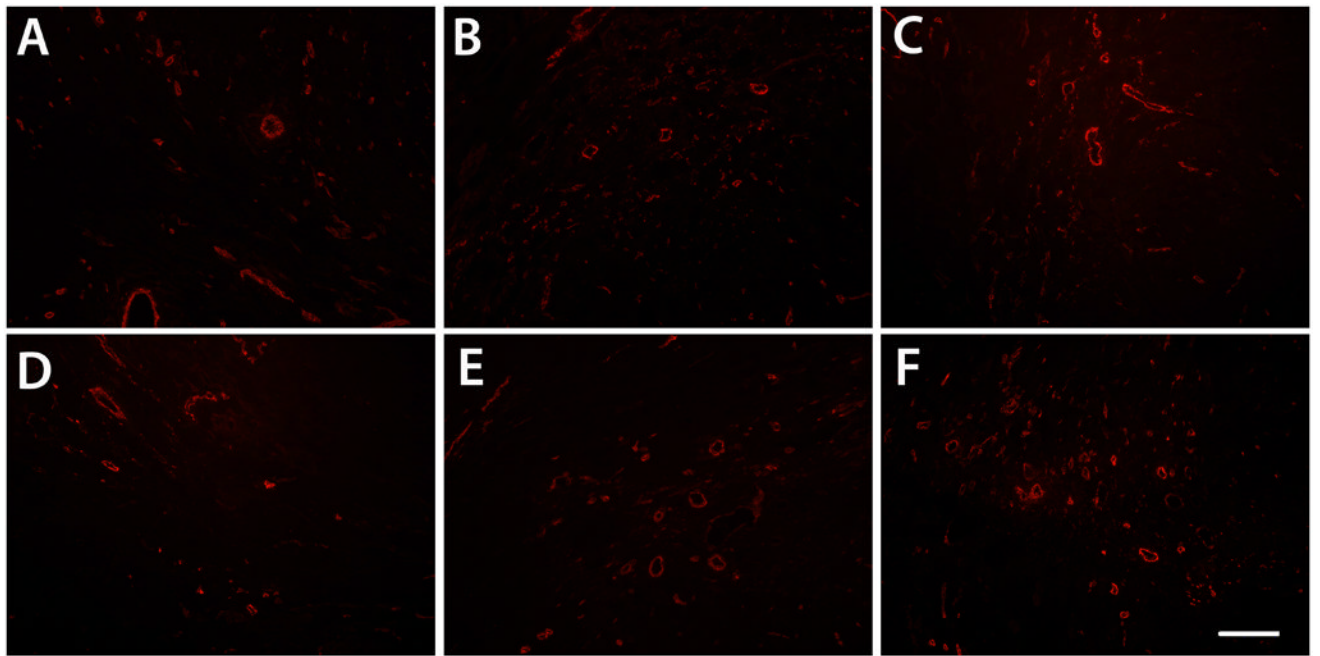


Figure 6. Neovascularization. Arterioles (red) in infarct regions of animals injected with bFGF in PPM (A), bFGF in collagen (B), bFGF in saline (C), PPM (D), collagen (E), and saline (F). Scale bar is 200 μm .

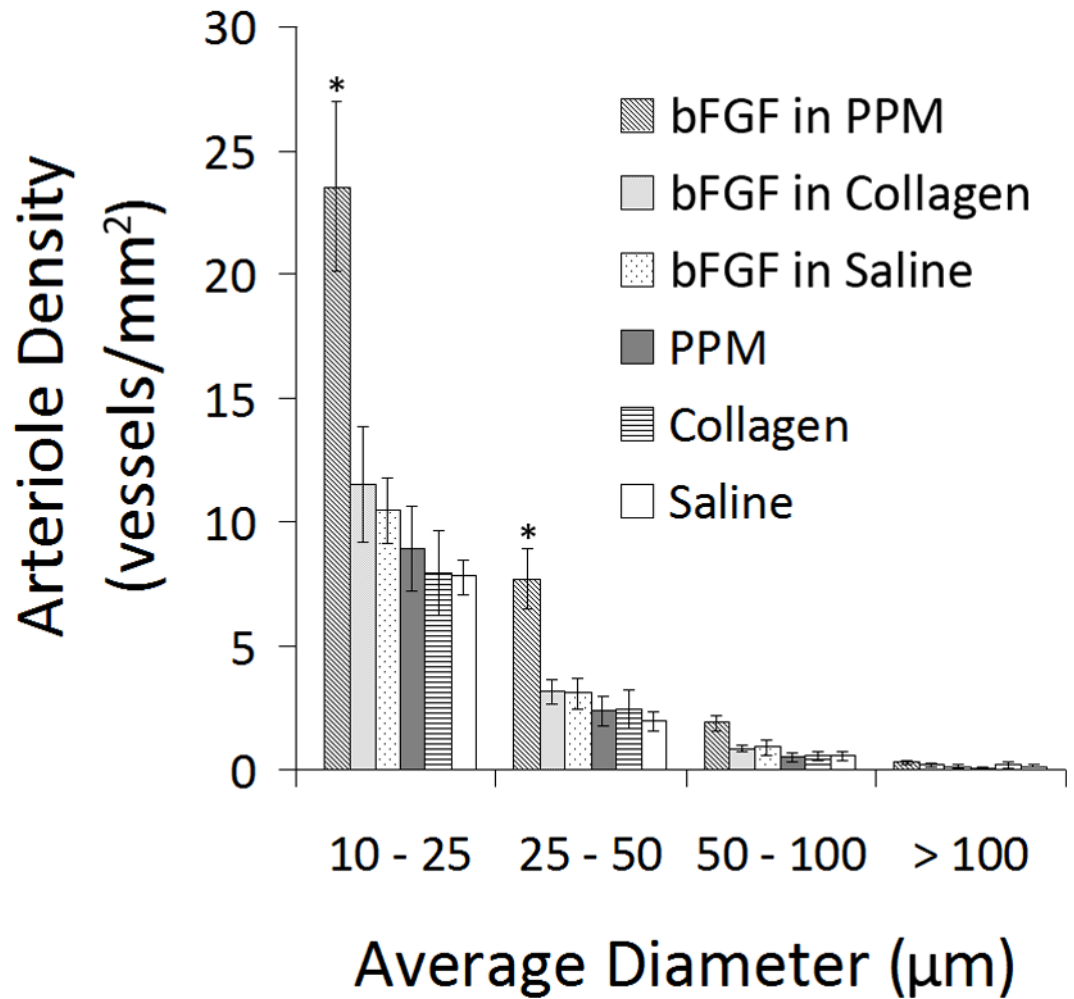


Figure 7. Arteriole density. Graphical representation of the arteriole density binned by vessel diameter. Majority of vessels are 10–25 µm in diameter. $*p < 0.05$ compared to all other treatment groups.

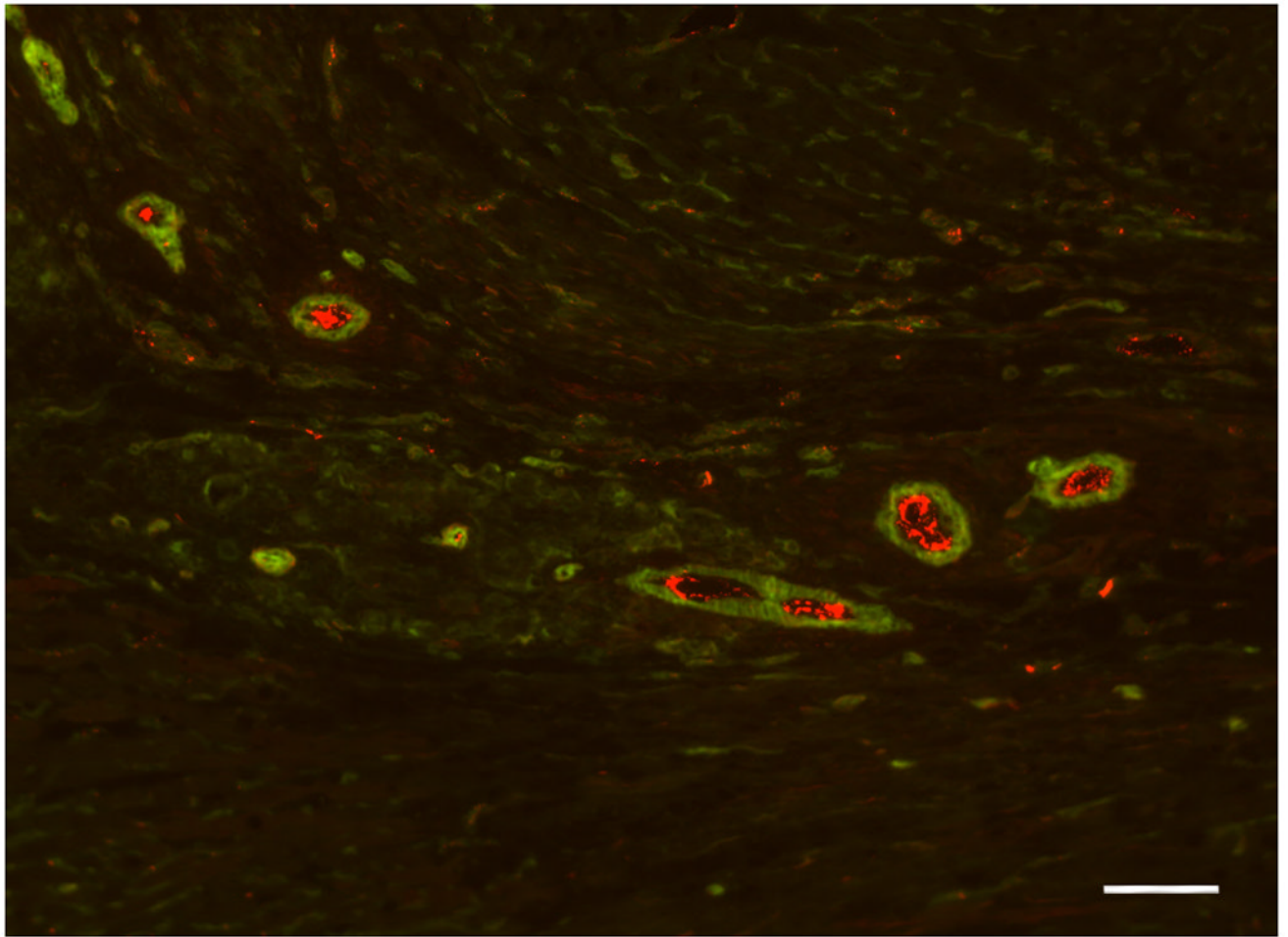


Figure 8. Functional vessels. Anastomosis is shown by red beads in vessels formed in the infarct of an animal injected with bFGF in PPM. Scale bar is 50 μm .